

~~CONFIDENTIAL~~

Copy
RM E57119

C2

NACA RM E57119

NACA

RESEARCH MEMORANDUM

INVESTIGATION OF TURBINES SUITABLE FOR USE IN A TURBOJET
ENGINE WITH HIGH COMPRESSOR PRESSURE RATIO AND LOW
COMPRESSOR-TIP SPEED

VIII - INTERNAL FLOW CONDITIONS OF A TWO-STAGE TURBINE
WITH A DOWNSTREAM STATOR

By Donald A. Petrash, Elmer H. Davison, and Harold J. Schum

Lewis Flight Propulsion Laboratory
Cleveland, Ohio

CLASSIFICATION CHANGED

LIBRARY COPY

NOV 11 1957

LANGLEY AERONAUTICAL LABORATORY
LIBRARY, NACA
LANGLEY FIELD, VIRGINIA

UNCLASSIFIED

To

By authority of TPA #33

CLASSIFIED DOCUMENT

Date 10-28-66

This material contains information affecting the National Defense of the United States within the meaning of the espionage laws, Title 18, U.S.C., Secs. 793 and 794, the transmission or revelation of which in any manner to an unauthorized person is prohibited by law.

ERK

NATIONAL ADVISORY COMMITTEE FOR AERONAUTICS

WASHINGTON

November 13, 1957

~~CONFIDENTIAL~~

UNCLASSIFIED

~~CONFIDENTIAL~~

NATIONAL ADVISORY COMMITTEE FOR AERONAUTICS

RESEARCH MEMORANDUM

INVESTIGATION OF TURBINES SUITABLE FOR USE IN A TURBOJET ENGINE
WITH HIGH COMPRESSOR PRESSURE RATIO AND LOW COMPRESSOR-TIP SPEED

VIII - INTERNAL FLOW CONDITIONS OF A TWO-STAGE TURBINE

WITH A DOWNSTREAM STATOR

By Donald A. Petrash, Elmer H. Davison, and Harold J. Schum

SUMMARY

As a part of a general study of obtaining high work output at low blade speeds with multistage turbines, a two-stage turbine with a downstream stator was experimentally investigated. The over-all performance of the turbine was lower than anticipated. Subsequently, a design-point survey was conducted to determine the interstage flow conditions of the turbine.

The survey revealed that the flow was underturned at the outlet of all blade rows, except for the downstream stator, with an area of severe underturning in the tip region of both rotors. In general, the Mach numbers throughout the turbine were higher than the design values. The downstream stator performed well, even though the flow conditions at the stator inlet were considerably different from design. The mismatch of the blade throat areas appears to have been the principal cause of the deviations of the flow conditions from design and the poor stage efficiencies. Downstream stator turbines would probably perform more efficiently if more current design methods that accounted for the three-dimensionality of the internal-flow conditions were employed.

INTRODUCTION

The NACA Lewis laboratory has been conducting a study of turbines to drive single-spool, high-pressure-ratio, low-blade-tip-speed compressors. One such turbine, consisting of two turbine stages followed by a downstream stator, was designed to meet the cruise requirements of a particular turbojet engine when the engine was operated at constant rotative speed (ref. 1). The aerodynamic blade design and over-all performance of this turbine are presented in reference 2. The aerodynamic design conditions

~~CONFIDENTIAL~~

UNCLASSIFIED

4370

CD-1

for the turbine are somewhat more critical than those for more conventional turbines in that the relative Mach number entering the first rotor hub was 0.793 and the turning at the hub was about 123° . The divergence of the inner shroud was also large, the half-cone angle being 27.6° (see fig. 2). The over-all performance investigation of the turbine indicated that, at equivalent design work and speed, design flow was obtained together with relatively good performance of the downstream stator. The downstream stator turned the flow leaving the last rotor in an axial direction with a recovery factor of 0.78. However, the over-all turbine efficiency at the design point was only 0.81 as compared with the design value of 0.86.

An experimental survey investigation was made near equivalent design work and speed in an effort to determine the internal flow conditions of the turbine and compare them with the design values. The purpose of this report is to present and discuss the results of this survey investigation and to point out some of the possible causes of the low design point turbine efficiency.

SYMBOLS

E	enthalpy drop (based on measured torque), Btu/lb
N	rotational speed, rpm
p'	total (stagnation) pressure, lb/sq ft
p'_x	rated total pressure, static pressure plus velocity pressure corresponding to axial component of velocity, lb/sq ft
T'	total (stagnation) temperature, $^\circ R$
w	weight flow, lb/sec
$\frac{wN}{608} \epsilon$	weight flow parameter based on equivalent weight flow and equivalent rotor speed, (lb)(rev)/sec ²
γ	ratio of specific heats
δ	ratio of inlet total pressure to NACA standard sea-level pressure of 2116 lb/sq ft

ϵ function of $\gamma, \frac{\gamma_{sl}}{\gamma_e}$

$$\left[\frac{\left(\frac{\gamma_e + 1}{2} \right) \frac{\gamma_e}{\gamma_e - 1}}{\left(\frac{\gamma_{sl} + 1}{2} \right) \frac{\gamma_{sl}}{\gamma_{sl} - 1}} \right]$$

4570

- η aerodynamic efficiency, based on measured total temperature
- η_x rating efficiency, ratio of actual turbine work (based on torque measurements) to ideal turbine work (based on exit pressure $P_{6,x}^*$)
- θ_{cr} squared ratio of critical velocity at NACA standard sea-level temperature of 518.7° R

Subscripts:

- e engine operating conditions
- sl NACA standard sea-level conditions
- 0,1,2,3, instrumentation stations (see fig. 2)
- 4,5,6

APPARATUS AND INSTRUMENTATION

The experimental test installation used in this investigation is the same as used in reference 2. A photograph of the test setup is presented in figure 1. Figure 2 is a schematic diagram of the turbine showing the axial location of the measuring stations and the measurements made at each station. With the exception of the added survey probes, the instrumentation was the same as in reference 2.

At the inlet and the outlet of the first-stage stator and at the outlet of the second-stage stator (stations 1, 2, and 4, see fig. 2), radial measurements of total pressure, temperature, and flow angle were made by the use of a combination probe mounted in a remotely controlled moveable actuator at one circumferential location. At the outlet of the first-stage rotor (station 3) similar measurements were made at two circumferential locations. At the stator exits, the actuators were located midway between the wakes from two adjacent stator blades. At the rotor exits, actuators were located midway between the leading edges of two adjacent stator blades. At the inlet and the outlet of the downstream stator (stations 5 and 6), circumferential as well as radial measurements were made with a single actuator at each station. These two probe actuators were mounted on a remotely controlled moveable survey pad (fig. 1) so that two full blade passages could be surveyed.

Radial static-pressure distributions at measuring stations 1 to 6 were also obtained by replacing the combination probes with static-pressure wedges. A photograph of both types of survey probe used for this investigation is presented in figure 3.

METHODS AND PROCEDURE

The turbine was operated near the equivalent design operating point (equivalent speed of 3027 and an equivalent work output of 33.06 Btu/lb based on torque measurements). The turbine-inlet total pressure p_0' was nominally 35 inches of mercury absolute and the inlet total temperature T_0 was maintained at 700° R. The over-all performance map for the subject turbine is reproduced from reference 2 as figure 4. Shown on this figure are the turbine equivalent design point and the equivalent operating point at which these survey data were obtained.

The indicated pressure and temperature readings obtained from the combination probes were corrected for Mach number effects. At the first-stage rotor outlet, the measurements from the two radial surveys were arithmetically averaged to obtain a single radial trace. At the downstream-stator inlet and outlet, a circumferential survey was made at 15 radii corresponding to $2\frac{1}{2}$, 5, 10, 15, 20, 30, 40, 50, 60, 70, 80, 85, 90, 95, and $97\frac{1}{2}$ percent of annular area. In order to obtain a single radial trace for the stage performance calculations at these two measuring stations, a circumferential average of the measurements was made at each radius. As a substitute for a Mach number correction for the indicated pressures obtained from the static-pressure wedges, the radial distributions were shifted so that the wedge values near the hub agreed with those obtained from the hub-wall static taps shown in figure 2.

Because of the difficulty in obtaining precise interstage flow measurements, the succeeding data should not be interpreted as an absolute measure of the parameters presented; however, it is felt that the trends are representative of the interstage flow conditions.

RESULTS AND DISCUSSION

The results of the survey investigation at equivalent design work and speed are presented and discussed in terms of individual stage efficiency and work parameter as well as stage flow angles and Mach numbers. The results obtained are compared with the design values in an effort to evaluate the interstage performance characteristics of the turbine.

Stage Efficiency And Work Output

Figure 5 presents the radial variation of stage and over-all efficiency η (based on measured temperatures and pressures) and work output parameter $\Delta T'/T'$ with percent annular area. The mass-averaged values of the parameters are also presented on the ordinate of each curve. The mass-averaged value of the first stage efficiency is 0.853 (fig. 5(a)).

Regions of low efficiency exist near the hub and the tip of the blade row. The mass-averaged value of the second-stage efficiency is only 0.670. The radial variation of the second-stage efficiency also shows regions of lower efficiency near the hub and the tip. The mass-averaged values of over-all turbine efficiency based on the flow conditions at the second-rotor outlet and the downstream-stator outlet are 0.788 and 0.771, respectively. The difference in these two efficiencies (0.017) measures the effect on the turbine aerodynamic efficiency of the total-pressure loss across the downstream stator. The over-all turbine efficiency, obtained from the over-all performance investigation, at the equivalent survey operating point was 0.81 (see fig. 4) based on torque measurements. This compares with 0.771 (based on measured temperatures and pressures) obtained from the survey investigation. This difference is an indication of the accuracy of the survey instrumentation.

The mass-averaged values of the stage work parameter for the first and second stages are 0.1613 and 0.1066 (fig. 5(b)). The over-all value of the mass-averaged work parameter, based on turbine-inlet and downstream-stator-outlet measurements, is 0.2497. These values correspond to the first and second stages producing 64.4 and 35.6 percent of the over-all turbine work output, respectively. These values are reasonably close to the design values of 67 and 33 percent for the first and second stages, respectively.

First-Stage Performance

The variation of the absolute and relative flow angles and Mach numbers with percent annular area is presented in figure 6. The radial variation of the design values (obtained from the design velocity diagrams of ref. 2) are also shown. The variation of the absolute flow angle at the first-stator outlet (fig. 6(a)) indicates that the flow was underturned from design by about 6° to 10° over most of the blade span. The relative flow angle indicates that a negative angle of incidence (herein, angle of incidence is defined as the deviation from the design angle) was present on the first rotor, which varied from 0° at the tip to 14° at the blade hub. The Mach numbers at the first-stator outlet (fig. 6(b)) were less than design near the hub and greater than design near the tip. These Mach number and flow angle data indicate that the throat area near the hub of the first-stage rotor is too small, whereas in the tip region, the area is too large. Possibly, contributing to the oversize area at the rotor tip is the relief in the outer casing that provides clearance over the rotor that was not accounted for in the turbine design (see schematic diagram, fig. 2). The relative flow angle at the first-rotor outlet was underturned from design on the order of 0° to 7° over most of the blade span with a condition of extreme underturning in the tip region, an indication that the flow separates from the rotor-blade suction surface in this region.

A contributing factor to the low efficiency observed in the first-stage hub region (fig. 5(a)) may be the large divergence of the inner wall (the cone half-angle of the inner wall is 27.6°). The region of low efficiency observed in the first-stage tip region is similar to that observed in the turbine of reference 3. Further investigation of that turbine revealed that when the rotor was shrouded to reduce the tip clearance and the rotor throat area was decreased, an improvement in the tip performance was realized (ref. 4). Correspondingly, changing the first-rotor throat-area distribution (decreasing the tip throat area and increasing hub throat area) and shrouding the blades of the subject turbine to reduce the large tip clearance (0.100 in.) should result in flow conditions closer to design with an attendant improvement in the first-stage performance.

Second-Stage Performance

The second-stage stator operates with negative incidence on the order of 0° to 10° over the blade height as indicated by the absolute flow angle at the outlet of the first-stage rotor (fig. 6(a)). The absolute flow angle at the outlet of the second-stage stator (fig. 6(a)) indicates that the flow was underturned on the order of 2° to 10° over most of the blade height. The relative flow angle at the second-stator outlet indicates that large negative angles of incidence were present on the hub section of the second-stage rotor and large positive incidence angles in the tip region. Over the blade span, the relative flow at the second-rotor outlet was slightly underturned. The absolute and relative Mach numbers at the second-stage stator and rotor outlets (fig. 6(b)) were, in general, considerably higher than the design values.

These Mach number and flow angle data indicate that the effective throat area of the second-stage rotor is too large, especially near the tip region. Reduction of the rotor throat area should cause the flow to approach the design flow conditions more closely. As mentioned previously, the variation of efficiency in the second stage had characteristics similar to those of the first stage, although, the level of the second-stage efficiency is considerably lower. This is partly attributed to the poor flow conditions at the stage inlet and the mismatched stator and rotor throat areas in the second stage. It might be noted also that, if the total-pressure drop to the second-stator throat could be reduced by increasing the first-stage efficiency and improving the flow conditions into the second stator, the second-stator throat area could also be reduced, and, thus, more exit turning could be obtained from the blade row.

Downstream-Stator Performance

Figures 7 to 10 present the results of the radial and circumferential survey measurements taken at the downstream-stator inlet and outlet (stations 5 and 6, respectively; fig. 2). Indicated values of flow angle, temperature, total pressure, and static pressure are shown. Because of the difficulty in obtaining precise measurements, the succeeding data should be interpreted as a qualitative indication of the interstage flow patterns and not as a measure of the absolute values of the parameters presented.

Figure 7 shows the variation of the absolute flow angle at the stator inlet and, outlet, respectively. Comparison of the two parts of the figure indicates that the large radial and circumferential variations in flow angle existing at the stator inlet are reduced in passing through the stator. In the midportion of the blade span at the stator outlet, the flow angle is reasonably uniform and near axial, varying for the most part between $+5^{\circ}$ and -5° , whereas, at the stator inlet the angle varied between -10° and -30° . (Positive angles are measured in the direction of wheel rotation.)

The radial and circumferential variations of measured temperature at the stator inlet and outlet are shown in figure 8. The temperature variations at the stator inlet (fig. 8(a)) were greatly reduced in passing through the stator. The most noticeable change occurred in the mid- and tip-portions of the blade span. The apparent temperature rise from the downstream-stator inlet to outlet indicated on the contour plots (fig. 8) is a result of not applying a Mach number correction to the indicated temperature data, and may possibly be due to temperature errors caused by fluctuations or pulsations caused by the second rotor. The wake patterns, noticeable on figure 8(a), occur with a frequency equivalent to that of the second-stage stator blades.

Figure 9 presents the variations in total pressure at the downstream-stator inlet and outlet. A comparison of figures 9(a) and (b) reveals that although the magnitude of the variations at the outlet is approximately the same as at the inlet, the flow at the stator outlet does not exhibit the very abrupt variations that are present at the inlet. Wake patterns are also noticeable at the stator inlet (fig. 9(a)) and appear again to occur with the same frequency as the number of second-stage stator blades. The variations of static pressure at the stator inlet and outlet are presented in figure 10. The static-pressure variations at the downstream-stator inlet are probably caused by the stator itself. Practically no circumferential static-pressure variation was observed at the stator outlet (fig. 10(b)).

Figures 7 to 9 show that although considerable radial and circumferential variations of flow angle, temperature, and total pressure were

present at the entrance to the downstream stator, these variations were greatly reduced by the downstream stator. Even though the Mach numbers at the downstream-stator entrance were considerably higher than design and large flow variations existed at the inlet to the blade row, the stator performed well with a recovery factor of 0.78 at the equivalent design operating point (ref. 2).

CONCLUDING REMARKS

Incorporating downstream stators in the design of turbines appears feasible. The principal cause of the low turbine efficiency obtained with an experimental two-stage turbine with a downstream stator appears to be the mismatch of the blade throat areas. Higher turbine efficiency could probably have been obtained if more current design techniques, incorporating the three-dimensional effects had been available for design.

SUMMARY OF RESULTS

From an experimental equivalent design-point-survey investigation of a high-work-output, low-blade-tip-speed, two-stage turbine with a downstream stator conducted at inlet conditions of 35 inches of mercury absolute and 700° R, the following results were obtained:

1. The mass-averaged values of the first- and second-stage efficiencies were 0.853 and 0.670, respectively.
2. Underturning of the flow, except for the downstream stator, was noted at the outlet of all blade rows. An area of severe underturning was found in the tip region of both rotors.
3. In general, the Mach numbers throughout the turbine were higher than the design values.
4. The main deviations of the flow conditions from design and the poor stage efficiencies primarily resulted from the mismatch of the blade throat areas.
5. The downstream stator performed well, even though the flow conditions at the stator inlet were far from design.

Lewis Flight Propulsion Laboratory
National Advisory Committee for Aeronautics
Cleveland, Ohio, September 18, 1957

REFERENCES

1. English, Robert E., and Davison, Elmer H.: Investigation of Turbines Suitable for Use in a Turbojet Engine with High Compressor Pressure Ratio and Low Compressor-Tip Speed. III - Velocity-Diagram Study of Two-Stage and Downstream-Stator Turbines for Engine Operation at Constant Rotative Speed. NACA RM E52G15, 1952.
2. Davison, Elmer H., Petrash, Donald A., and Schum, Harold J.: Investigation of Turbines Suitable for Use in a Turbojet Engine with High Compressor Pressure Ratio and Low Compressor-Tip Speed. V - Experimental Performance of Two-Stage Turbine with Downstream Stator. NACA RM E55H16, 1955.
3. Davison, Elmer H., Schum, Harold J., and Petrash, Donald A.: Investigation of Turbines Suitable for Use in a Turbojet Engine with High Compressor Pressure Ratio and Low Compressor-Tip Speed. VI - Experimental Performance of Two-Stage Turbine. NACA RM E56E04, 1956.
4. Davison, Elmer H., Petrash, Donald A., and Schum, Harold J.: Investigation of Turbines Suitable for Use in a Turbojet Engine with High Compressor Pressure Ratio and Low Compressor-Tip Speed. VII - Experimental Performance of Modified Two-Stage Turbine. NACA RM E56H14a, 1956.

4370

CD-2

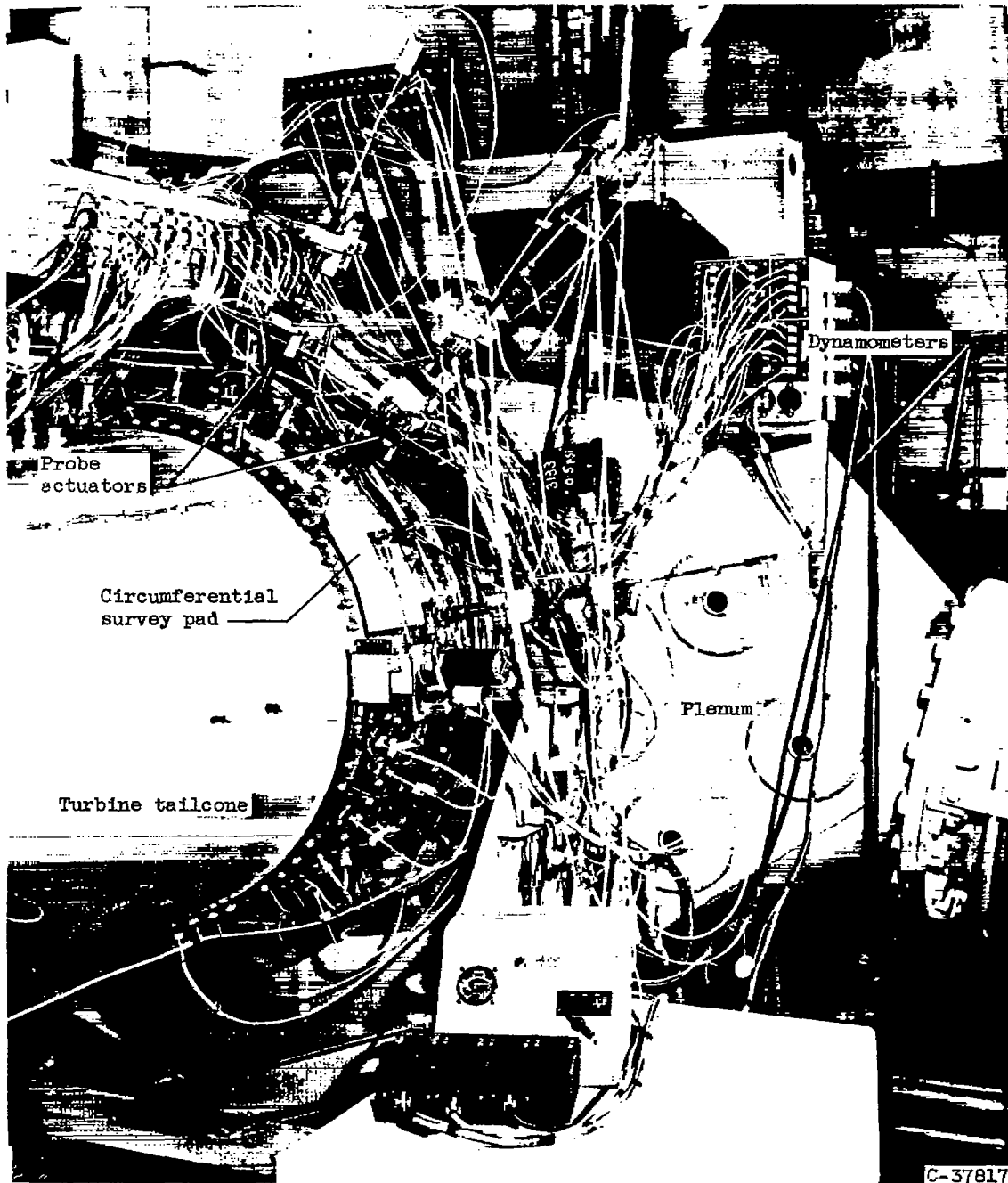


Figure 1. - Installation of turbine in full-scale turbine component test facility.

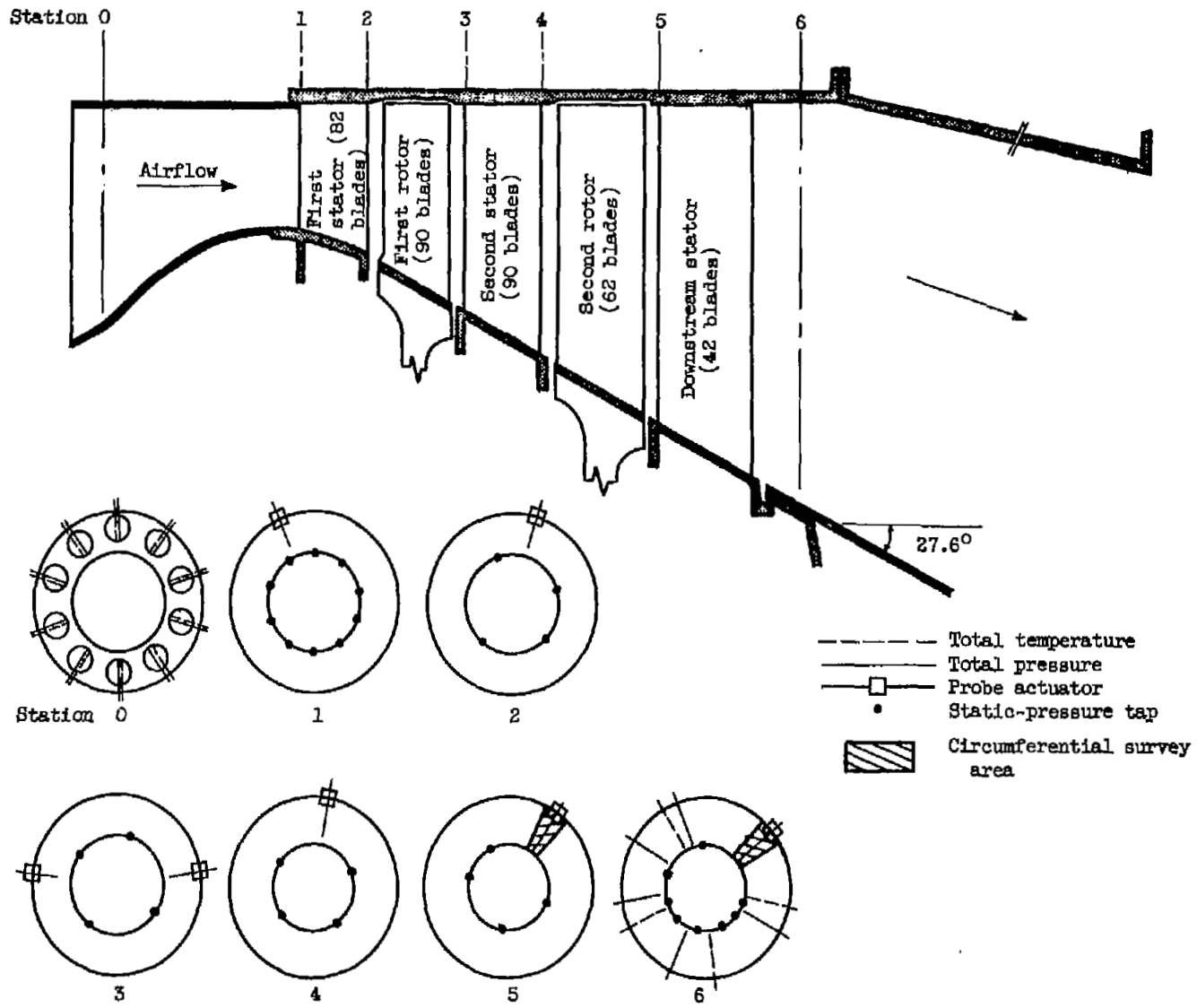
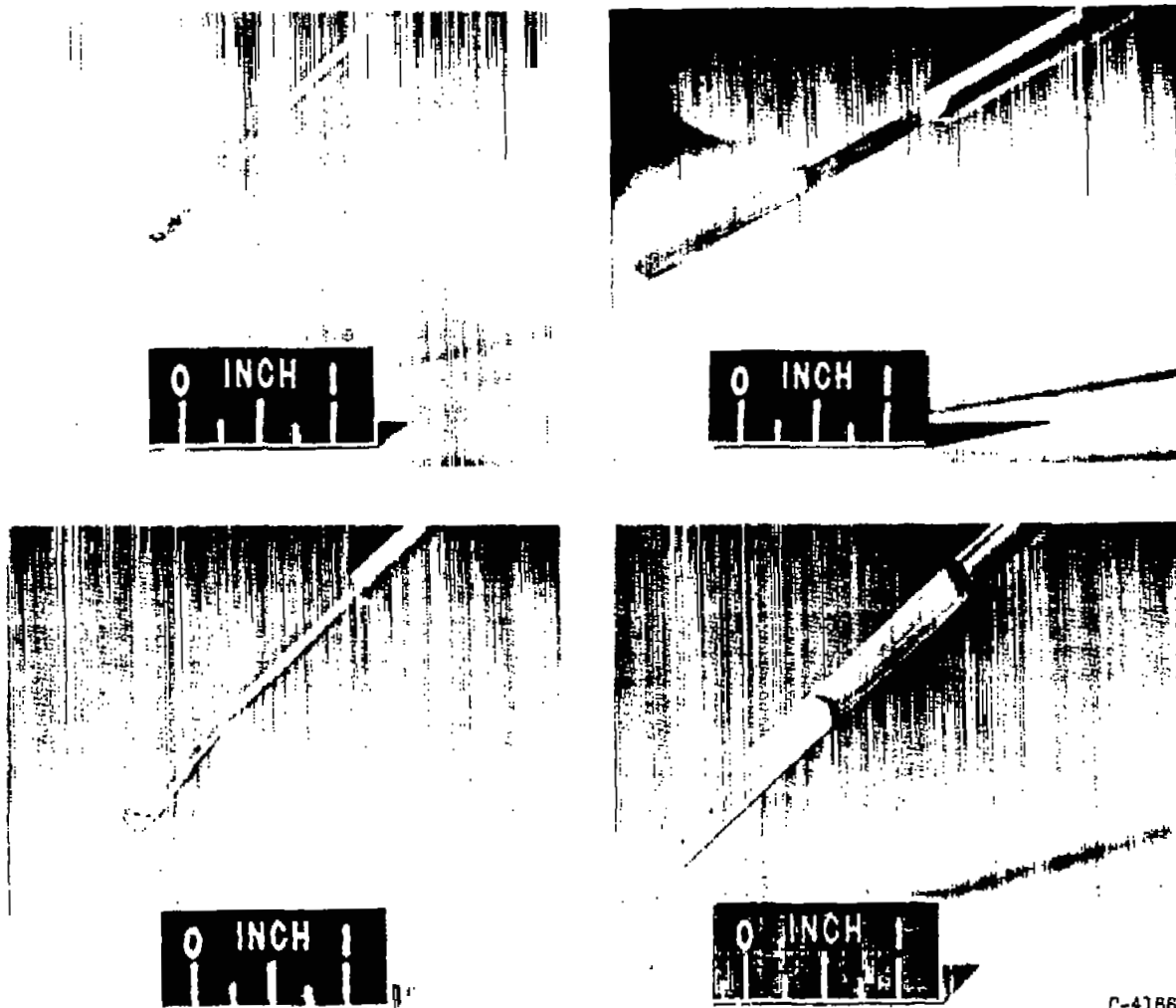


Figure 2. - Schematic diagram of turbine showing instrumentation.



(a) Combination total-pressure, total-temperature, and angle probe.

(b) Static-pressure wedge.

Figure 3. - Survey instruments.

C-41862

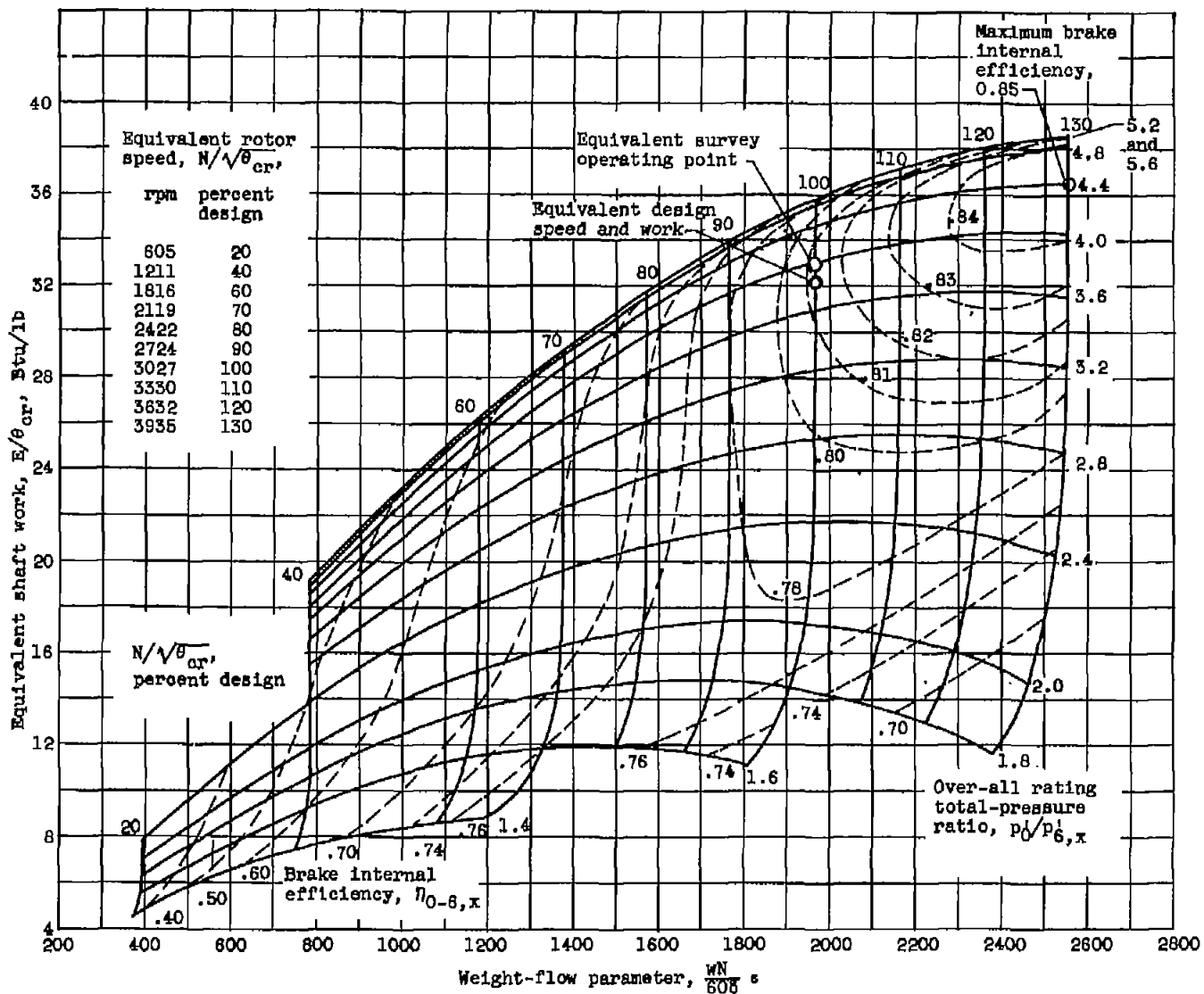
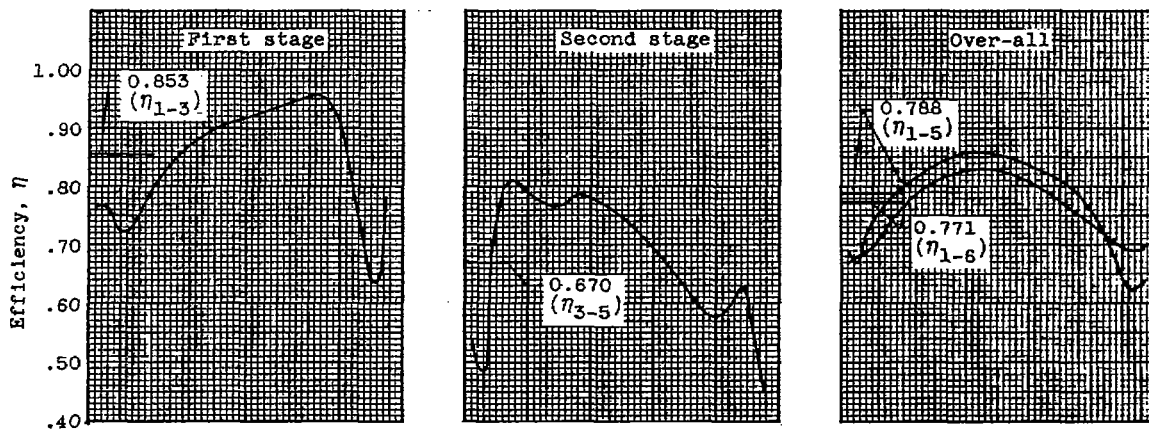
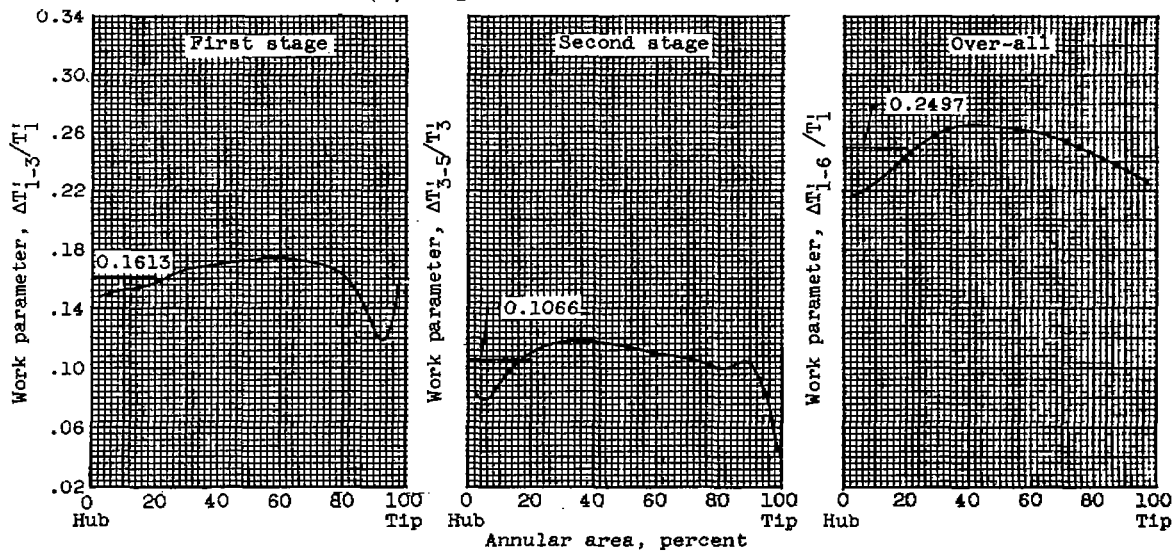


Figure 4. - Over-all performance of turbine. Turbine-inlet pressure, 35 inches of mercury absolute; turbine-inlet temperature, 700° R (ref. 2).

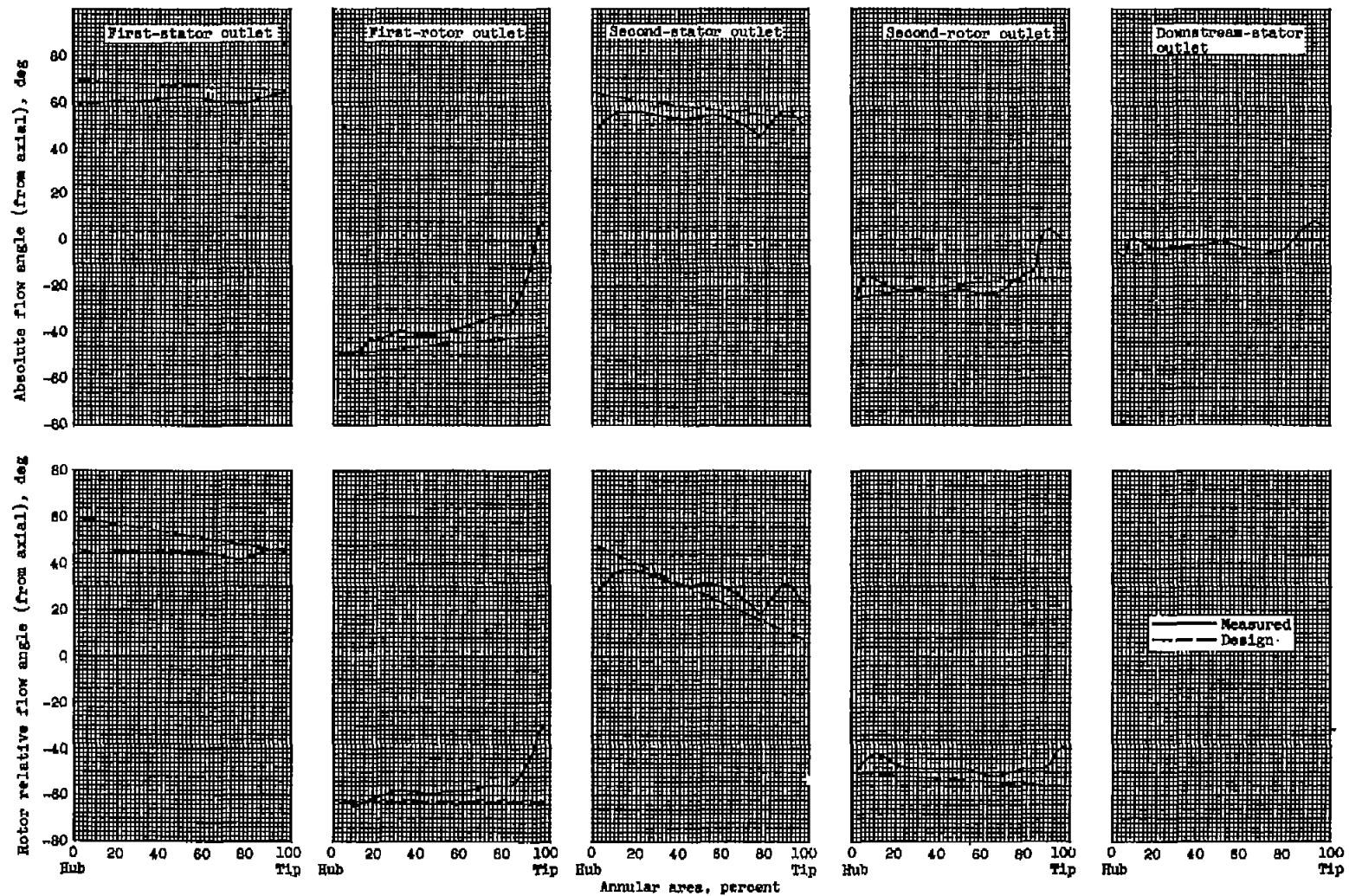


(a) Stage and over-all internal efficiencies.



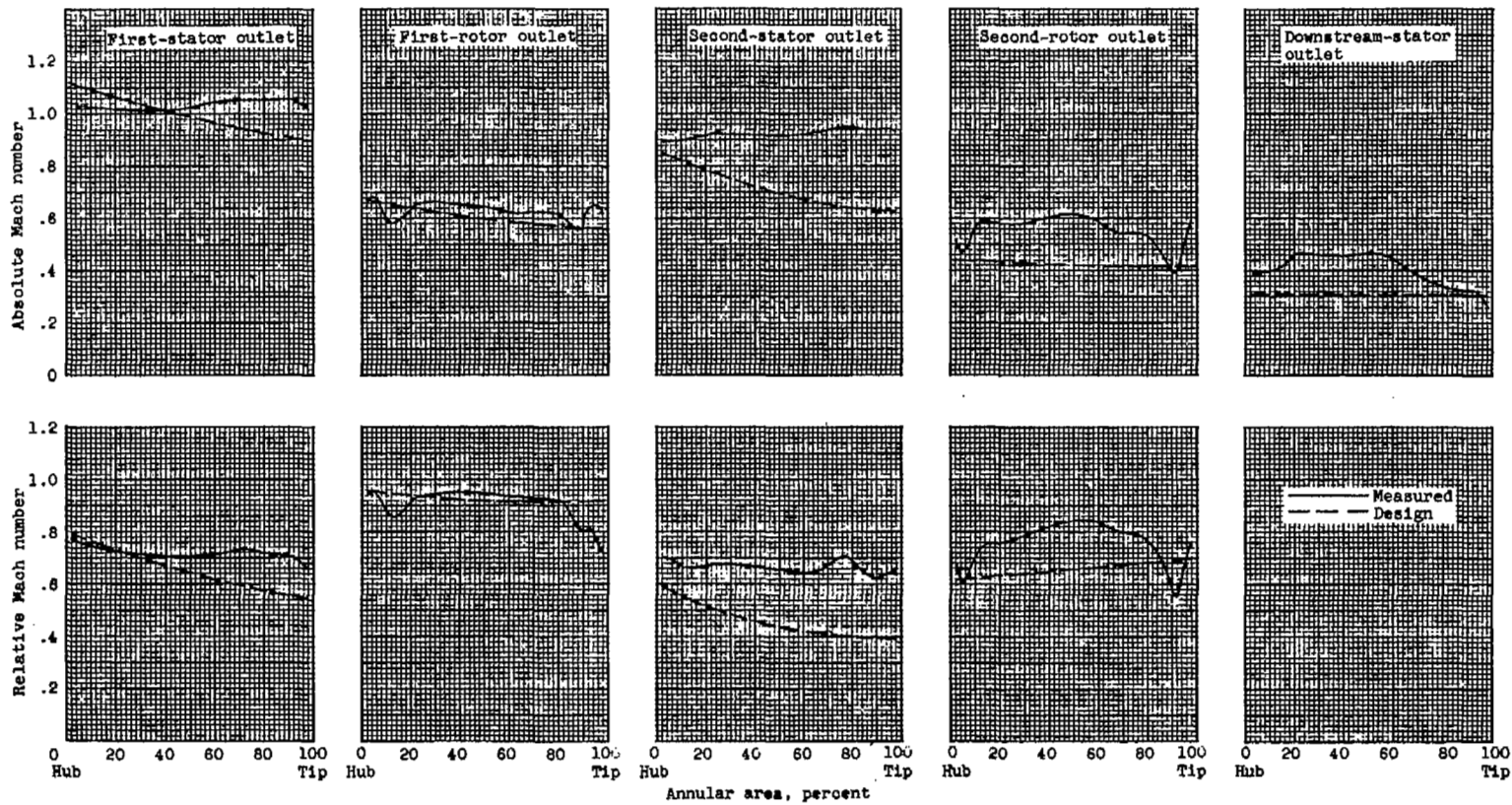
(b) Stage and over-all work parameters.

Figure 5. - Radial variation of work parameter and efficiency at design speed and work.



(a) Variation of absolute and relative flow angle with percent annular area.

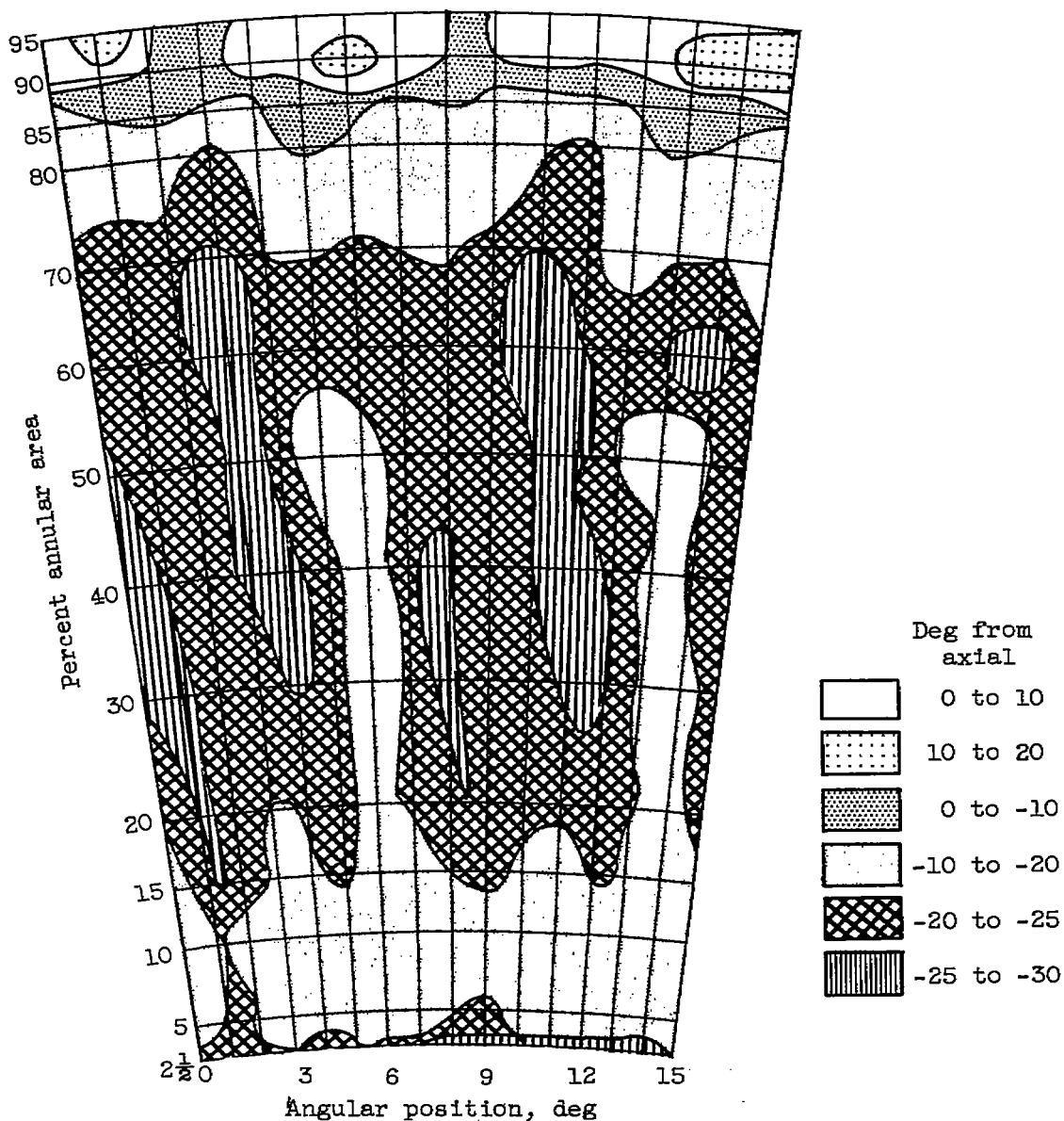
Figure 5. - Radial variation of absolute and relative flow angle and Mach number.



(b) Variation of absolute and relative Mach number with percent annular area.

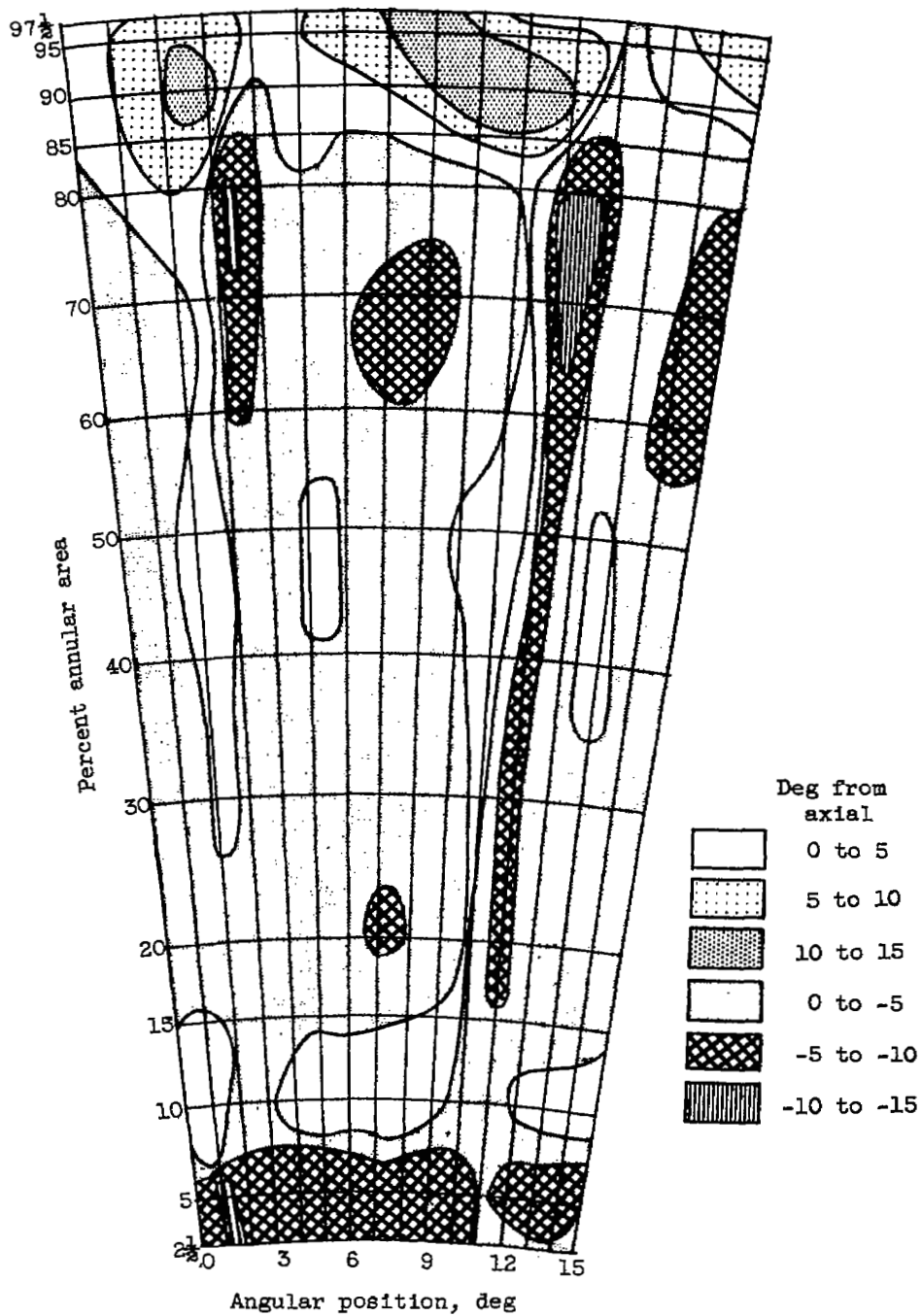
Figure 6. - Concluded. Radial variation of absolute and relative flow angle and Mach number.

CD-3 4370



(a) Inlet.

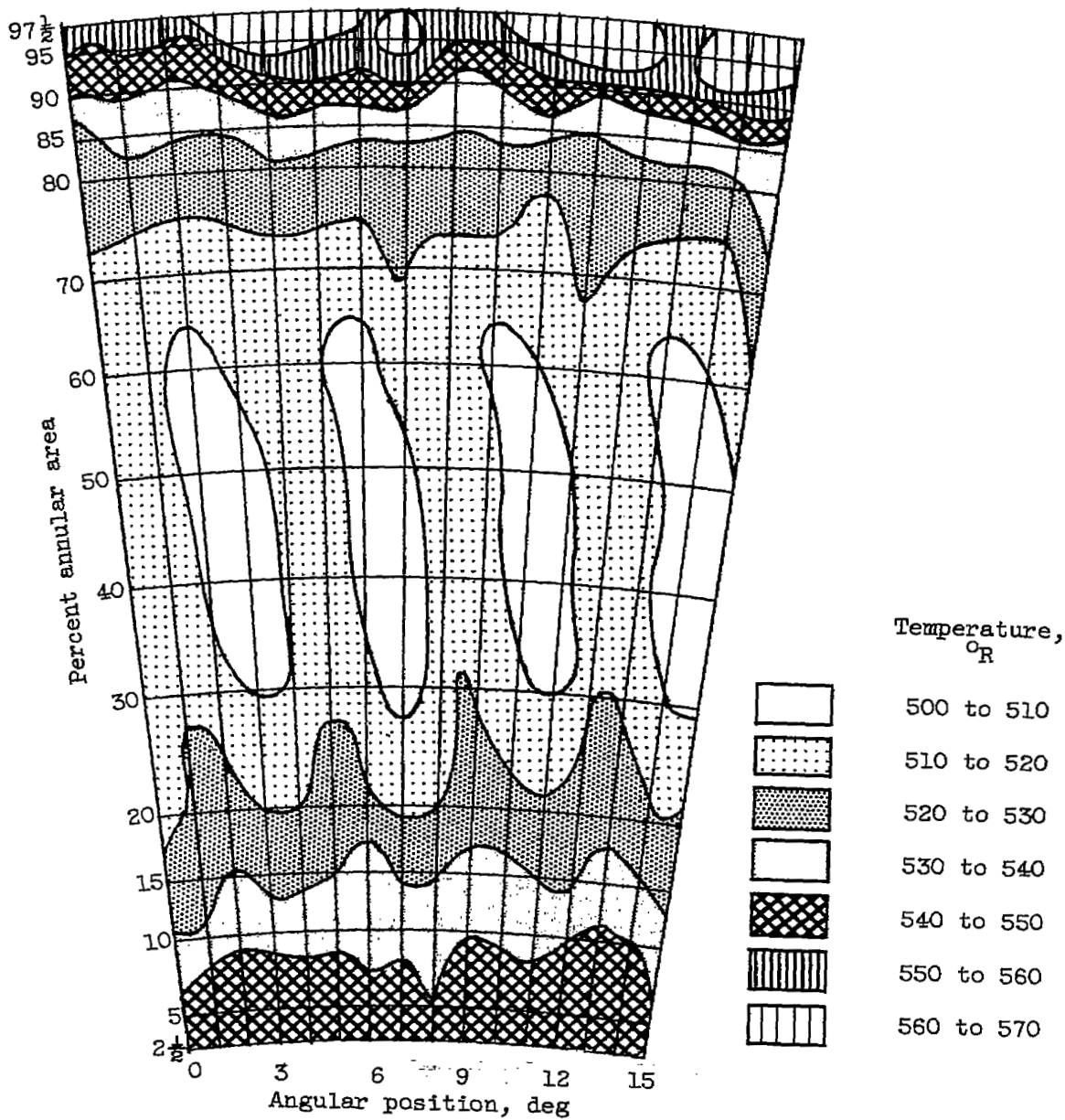
Figure 7. - Absolute flow angle distribution at downstream-stator inlet and outlet.



(b) Outlet.

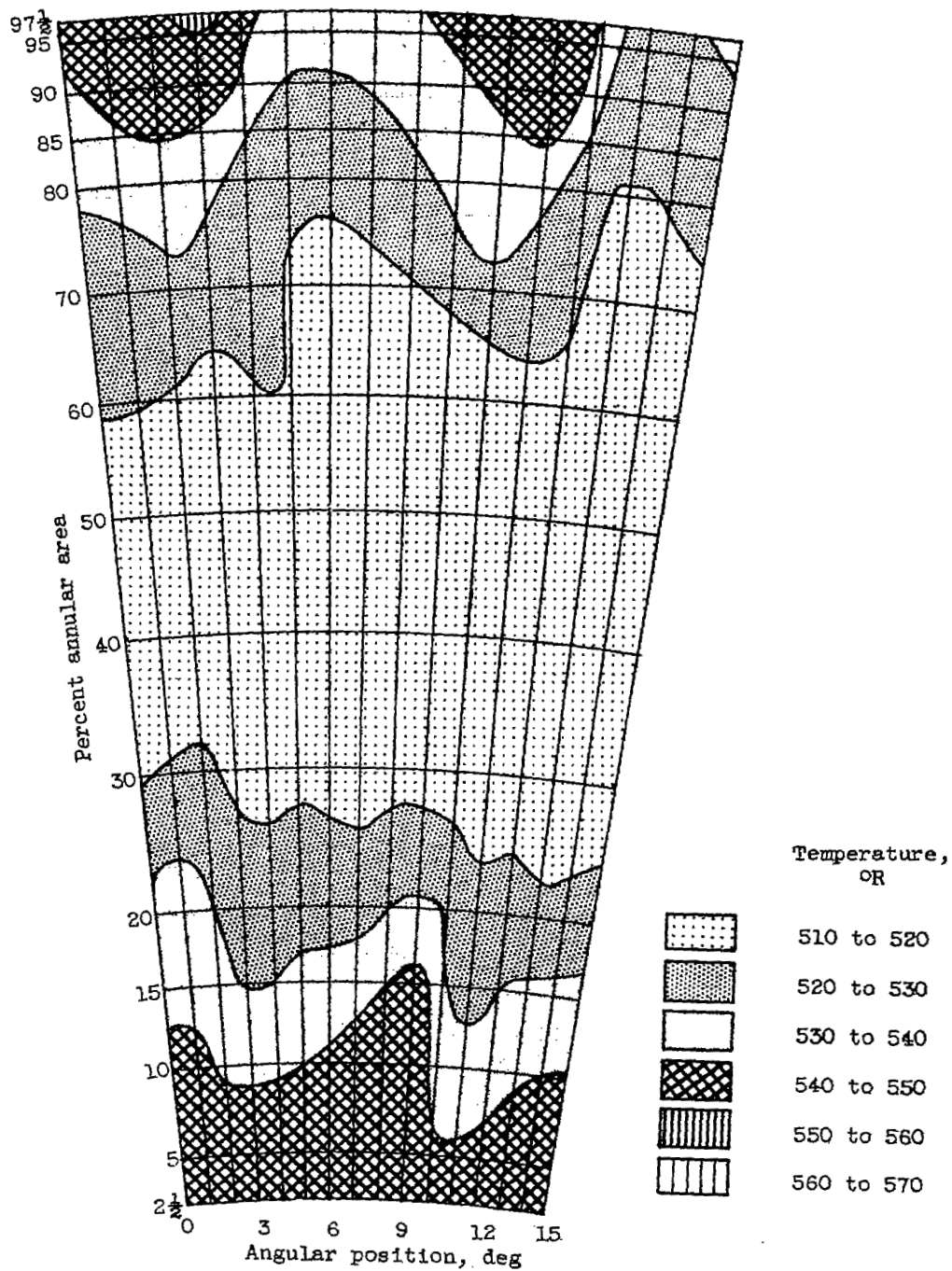
Figure 7. - Concluded. Absolute flow angle distribution at downstream-stator inlet and outlet.

CD-3 back 4370



(a) Inlet.

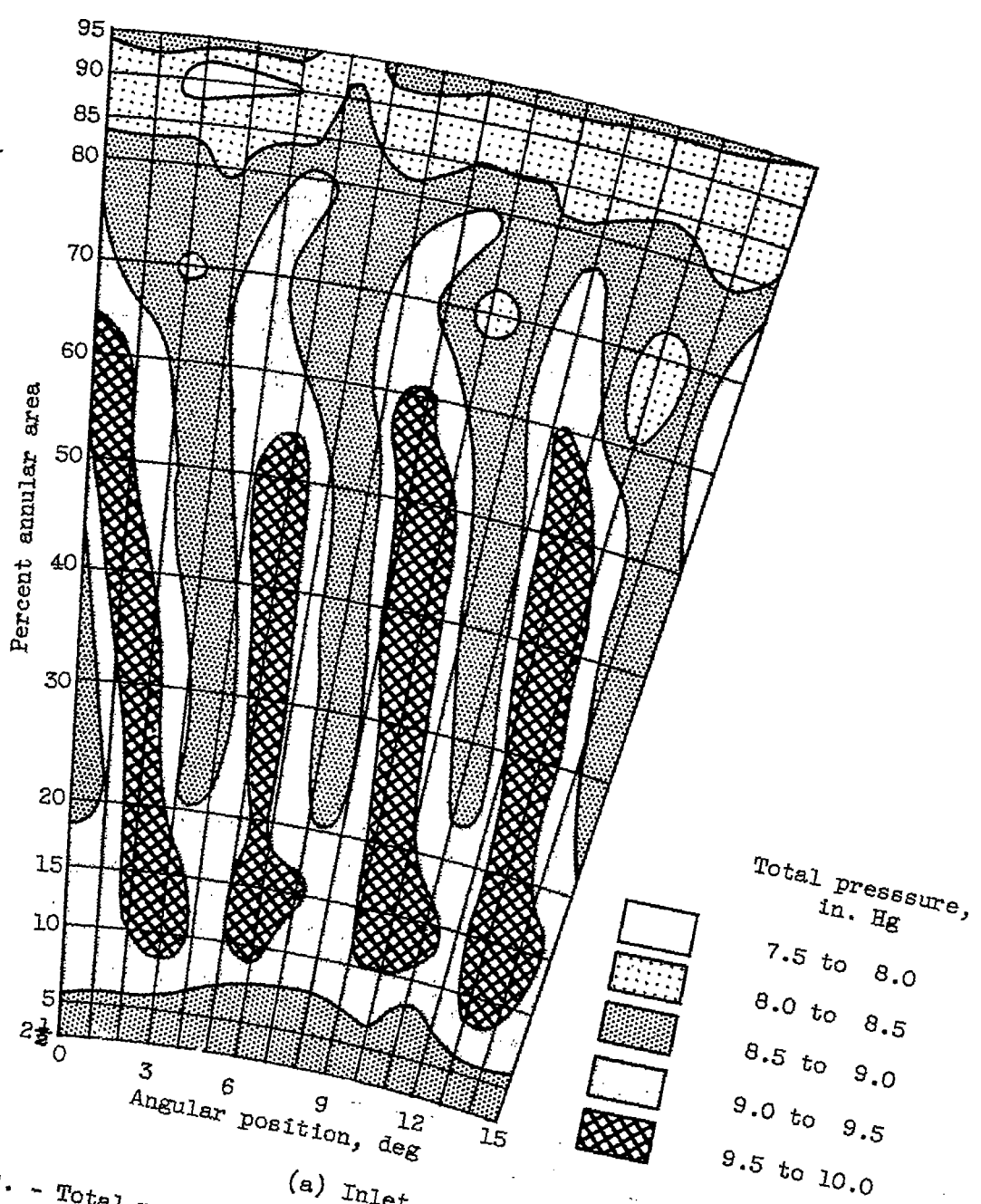
Figure 8. - Measured temperature distribution at downstream-stator inlet and outlet.



(b) Outlet.

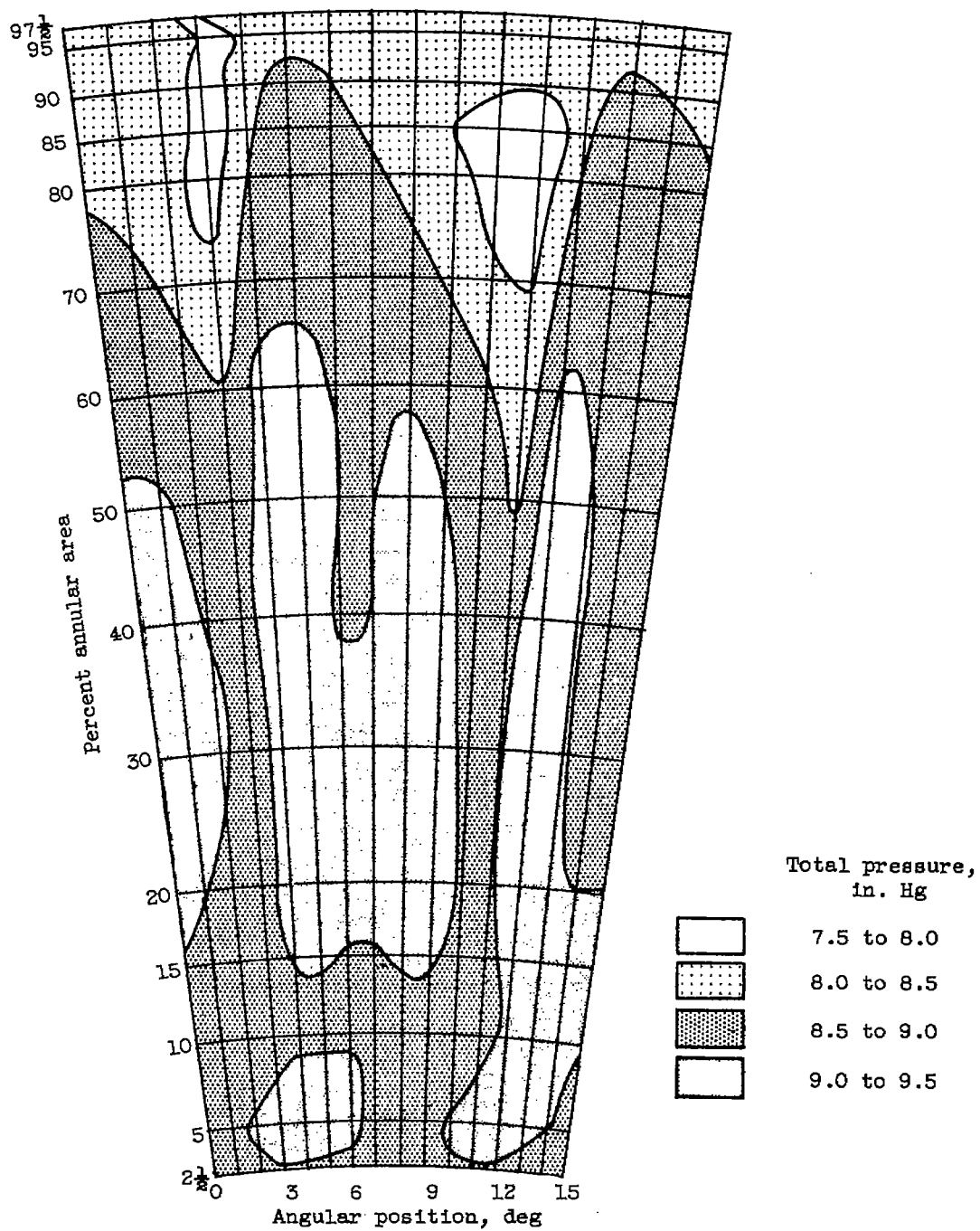
Figure 8. - Concluded. Measured temperature distribution at downstream-stator inlet and outlet.

4370



(a) Inlet.

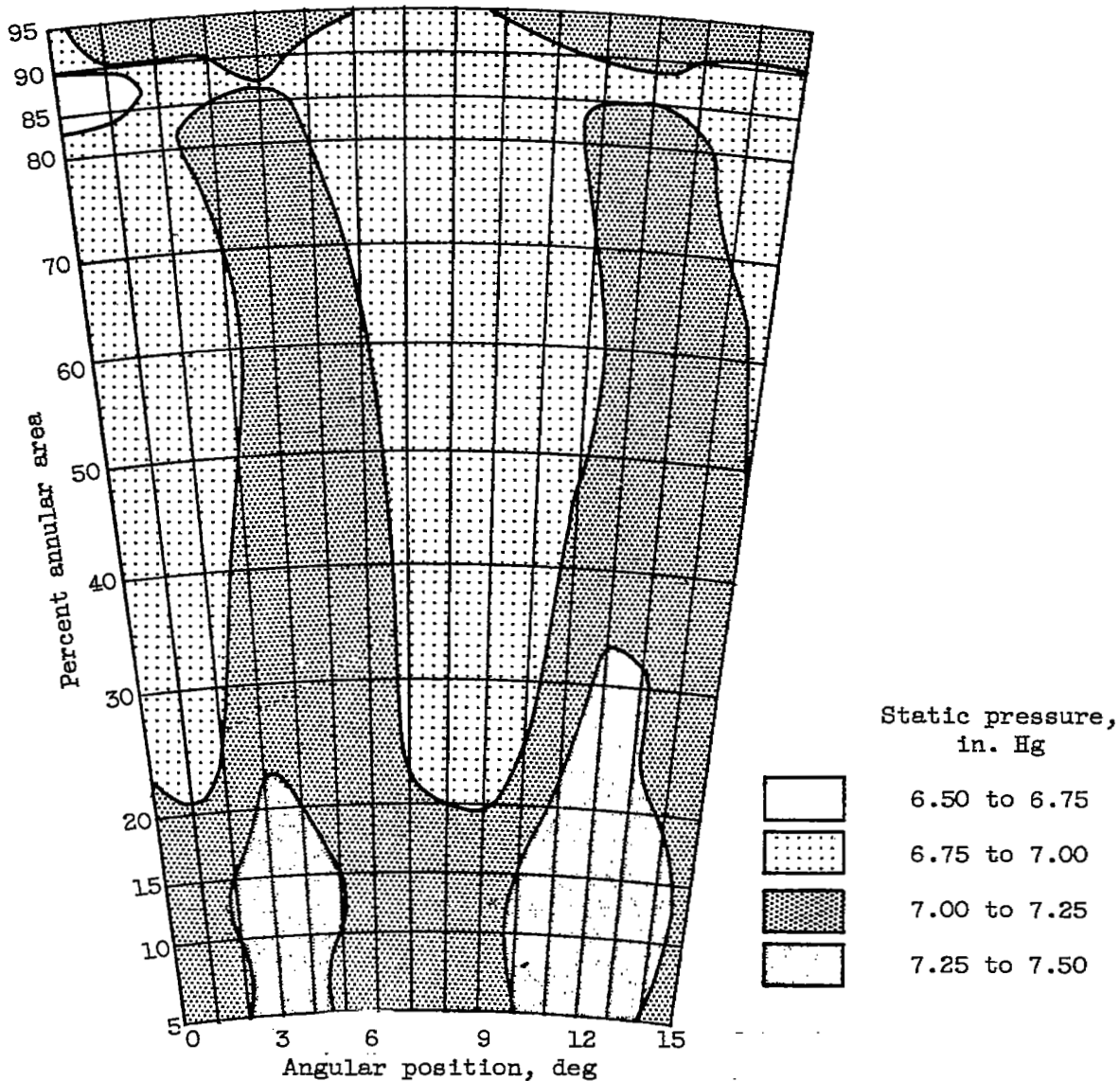
Figure 9. - Total-pressure distribution at downstream-stator inlet and outlet.



(b) Outlet.

Figure 9. - Concluded. Total-pressure distribution at downstream-stator inlet and outlet.

4370



(a) Inlet.

Figure 10. - Static-pressure distribution at downstream-stator inlet and outlet.

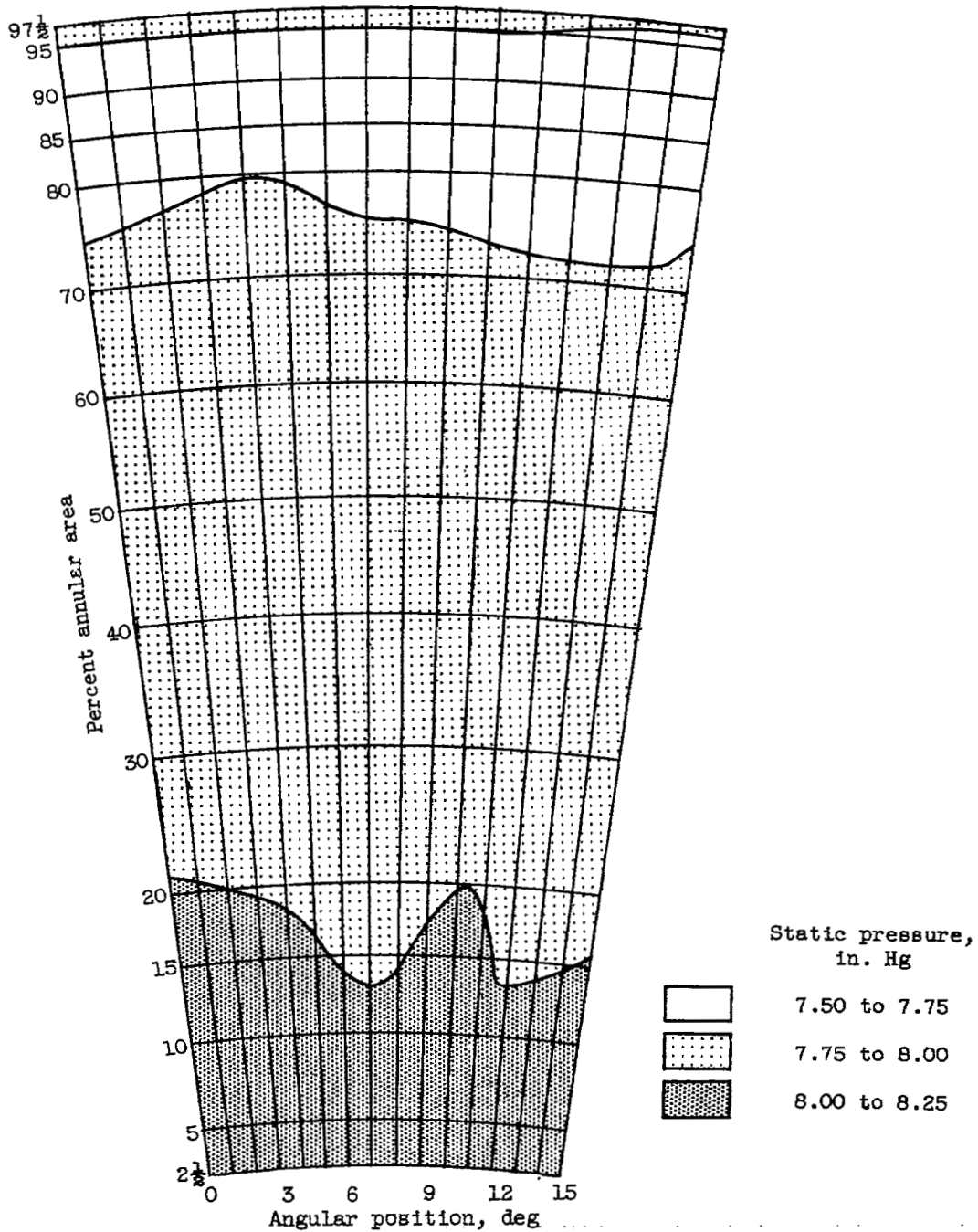


Figure 10. - Concluded. Static-pressure distribution at downstream-stator inlet and outlet.

[REDACTED]

NASA Technical Library
3 1176 01435 8809

[REDACTED]

[REDACTED]

[REDACTED]

[REDACTED]

[REDACTED]